Development of Selective Bisubstrate-Based Inhibitors Against Protein Kinase C (PKC) Isozymes By Using Dynamic Peptide Microarrays

ARTICLE *in* CHEMBIOCHEM · AUGUST 2009

Impact Factor: 3.09 · DOI: 10.1002/cbic.200900199 · Source: PubMed

8 AUTHORS, INCLUDING:

Alex J Poot
VU University Medical Center
17 PUBLICATIONS **358** CITATIONS
SEE PROFILE

Riet Hilhorst
PamGene International BV
162 PUBLICATIONS **2,110** CITATIONS
SEE PROFILE

Rob Ruijtenbeek
PamGene
80 PUBLICATIONS **648** CITATIONS
SEE PROFILE

Rob M J Liskamp
University of Glasgow
412 PUBLICATIONS **10,893** CITATIONS
SEE PROFILE

CHEMBIOCHEM

DOI: 10.1002/cbic.200900199

Development of Selective Bisubstrate-Based Inhibitors Against Protein Kinase C (PKC) Isozymes By Using Dynamic Peptide Microarrays

Alex J. Poot,[a] Jeroen van Ameijde,[a] Monique Slijper,[b] Adriënne van den Berg,[c] Riet Hilhorst,[c] Rob Ruijtenbeek,[c] Dirk T. S. Rijkers,[a] and Rob M. J. Liskamp*[a]

Kinase inhibitors are increasingly important in drug development. Because the majority of current inhibitors target the conserved ATP-binding site, selectivity might become an important issue. This could be particularly problematic for the potential drug target protein kinase C (PKC), of which twelve isoforms with high homology exist in humans. A strategy to increase selectivity is to prepare bisubstrate-based inhibitors that target the more selective peptide-binding site in addition to the ATP-binding site. In this paper a generally applicable, rapid methodology is presented to discover such bisubstrate-based leads. Dynamic peptide microarrays were used to find peptide-binding site inhibitors. These were linked with chemoselective click chemistry to an ATP-binding site inhibitor, and this led to novel bisubstrate structures. The peptide microarrays were used to evaluate the resulting inhibitors. Thus, novel bisubstrate-based inhibitors were obtained that were both more potent and selective compared to their constituent parts. The most promising inhibitor has nanomolar affinity and selectivity towards PKCθ amongst three isozymes.

Introduction

Kinases are widely recognised as important drug targets involved in many serious diseases, such as cancer and diabetes.[1,2] These phosphorylating enzymes play a pivotal role in cellular signal transduction, and many diseases are characterised by abnormalities in a kinase or its expression level. It is no surprise, therefore, that kinase inhibitors are sought-after medicinal leads, and indeed a sizeable number of them have reached the drug market.[2] However, most current compounds only bind to the ATP-binding site of a kinase, which obviously often has large structural similarity to the ATP-binding domains of other kinases. This could lead to decreased selectivity.[3]

It is possible to target the peptide-binding site by so-called pseudosubstrates, which are peptides derived from the kinase substrate in which the phosphate-accepting amino acid residue (serine/threonine) has been changed to an alanine residue; these have a substrate-like interaction with the active site without actually being a substrate.[4] However, (pseudo)substrate peptides often have significantly lower affinity compared to ATP-binding site inhibitors. To have both affinity and selectivity, so-called bisubstrate-based inhibitors have been designed and investigated that bind to both the ATP-binding site and the peptide-binding site of a kinase.[5] In these constructs, the ATP-binding site inhibitor part affords affinity and the peptide part affords selectivity. Successful examples of this approach include the oligo-arginine-linked ATP analogues,[6] the known pseudosubstrate kemptide linked to staurosporine,[7] the ATP-based tyrosine kinase inhibitors developed by Cole and co-workers,[8] the coupling of complex cyclic peptides obtained from phage display experiments to staurosporine,[9] the attachment of aromatic moieties that can function as ATP analogues to a peptide substrate for the Akt kinase,[10] and the conjugation of phenylpyrazolo-pyrimidine derivatives to a Src kinase substrate.[11] In all these studies increases in selectivity and affinity were observed, and this indicates the validity of the strategy.

In this paper a general approach (Figure 1) is described to find bisubstrate-based inhibitors of kinases by using dynamic peptide microarrays and the chemoselective Huisgen cycloaddition (the "click" reaction).[12] This versatile synthetic procedure can be carried out in the presence of a large variety of functional groups and allows the preparation of many different combinations of peptides, linkers and ATP-binding site inhibitors. Consequently, optimization of the resulting bisubstrate-based inhibitors is convenient. Peptide microarrays are used initially to discover peptide substrates with large affinity differences within a given set of kinases. Then, these substrates are

[a] A. J. Poot, Dr. J. van Ameijde, Dr. D. T. S. Rijkers, Prof. Dr. R. M. J. Liskamp
Department of Medicinal Chemistry and Chemical Biology
Utrecht Institute for Pharmaceutical Sciences, Faculty of Science
Utrecht University
Sorbonnelaan 16, 3584 CA, Utrecht (The Netherlands)
Fax: (+31) (0)30 2536655
E-mail: r.m.j.liskamp@uu.nl

[b] Dr. M. Slijper
Biomolecular Mass Spectrometry and Proteomics Group
Utrecht Institute for Pharmaceutical Sciences and
Bijvoet Centre for Biomolecular Research, Faculty of Science
Utrecht University
Sorbonnelaan 16, 3584 CA, Utrecht (The Netherlands)

[c] A. van den Berg, Dr. R. Hilhorst, Dr. R. Ruijtenbeek
Pamgene International BV
P.O. Box 1345, 5200 BJ, 's-Hertogenbosch (The Netherlands)

Supporting information for this article is available on the WWW under http://dx.doi.org/10.1002/cbic.200900199.

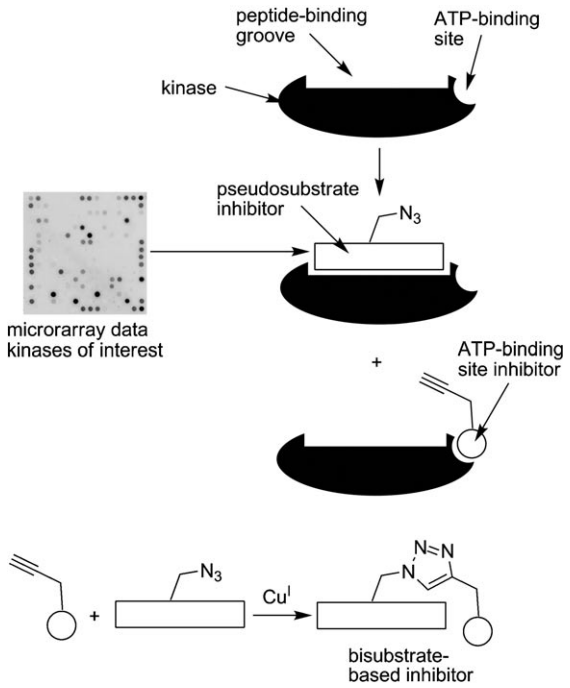

Figure 1. Design of novel bisubstrate-based kinase inhibitors.

transformed into pseudosubstrates that are linked chemoselectively to an ATP-binding site inhibitor either directly or through a spacer. Comparison of the inhibitory activity and selectivity of the resulting bisubstrates as well as their constituent parts is then achieved efficiently by using the microarrays.

Clearly, the dynamic peptide microarrays were crucial in this approach. PamChip STK (serine/threonine kinase) microarrays that were developed by Pamgene International BV ('s-Hertogenbosch, The Netherlands) were used, on which hundreds of peptidic serine/threonine kinase substrates can be immobilised in discrete spots.[13] All peptides are derived from known endogenous kinase substrate proteins. To detect phosphorylation events, a mixture of antiphosphoserine/antiphosphothreonine antibodies and generic fluorescent secondary antibodies was added to a solution of the kinase of interest, with ATP and cofactors. The porous material onto which the peptides are immobilised allows an analyte mixture to be pumped up and down; this allows for efficient mixing, offers the possibility to monitor the increase in fluorescence in real time and generates kinetic data (K_M, k_{cat}, K_i) of the phosphorylation process. After quantification, comprehensive substrate–activity data against all substrates can be obtained for the kinase of interest. A recent paper described the application of these microarrays to thoroughly investigate protein kinase A (PKA) with respect to substrate specificity, kinetics and inhibition.[13d] The data that were obtained in that study correlated well with literature data; this demonstrates the applicability of microarrays as a reliable and convenient kinase assay platform.

The discovery strategy was applied to the challenging protein kinase C (PKC) family. These enzymes are involved in diseases such as cancer and diabetes and have attracted attention as potential drug targets for a long time.[14,15] Homology between the twelve isoforms of the PKC family is very high in particular for their catalytic domains, that is, up to 80%,[16,17] and selective inhibition is a difficult issue. As a consequence, uncovering selective bisubstrate-based inhibitors is very challenging and could serve as an excellent proof-of-principle of our approach.

Results and Discussion

Substrate profiling and selection

Three PKC isozymes were selected for substrate profiling, one from each of the three PKC subfamilies, namely PKCα, PKCζ and PKCθ. PKCα is a subject of cancer-related research because of its ability to regulate phospholipase D[18] and its important role in haematology.[19] PKCζ was selected as a member of the atypical PKCs, and is known to be involved in long-term memory processes[19] and the immune system.[21] Finally, PKCθ was chosen because this kinase has recently emerged as a pharmacological target in human T cell leukaemias.[10] It should be noted that the substrate sequence specificity of several PKC isozymes has been studied in a large combinatorial study by Nishikawa et al.,[22] however the pharmacologically interesting PKCθ isozyme was not included in that study.

In the screening experiment, a cocktail of three antiphosphoserine and antiphosphothreonine antibodies was used because, to the best of our knowledge, no currently available antibody is completely impervious to the peptide sequences flanking the phosphorylated serine or threonine residue. For detection, fluorescently labelled secondary antibodies were added. The cocktail applied here was selected to give a strong fluorescent signal for all substrates on the microarray. The increase in fluorescence was monitored for each substrate (Figure 2A) and plotted against time (Figure 2B). The slope of each phosphorylation curve was calculated and converted into an initial velocity (v_{in}). This was carried out in triplicate for all three PKC isozymes (Figure 2C).

Analysis of the data revealed that 20 peptides on the array were phosphorylated by the isozymes (Figure 2D, Table 1). Comparison with commonly used kinase databases revealed overlap with the substrate peptides found in this study, and several previously unknown substrate sequences were found as well. Gratifyingly, from these data it followed that a number of substrate peptides showed selectivity with respect to phosphorylation by these three PKC isozymes.

For this study, the peptide EILSRRPSYRKIL, derived from the cAMP-responsive element binding protein[23] was selected as the basis for bisubstrate-based inhibitors because it combined good selectivity, in this case towards phosphorylation by PKCζ, with a high phosphorylation rate and therefore affinity. Additionally, the phosphorylation site of this peptide by PKC isozymes is known, which makes selecting the correct serine residue to be replaced by an alanine amino acid as well as determining the attachment point for the ATP-binding site inhibitor convenient (vide infra).

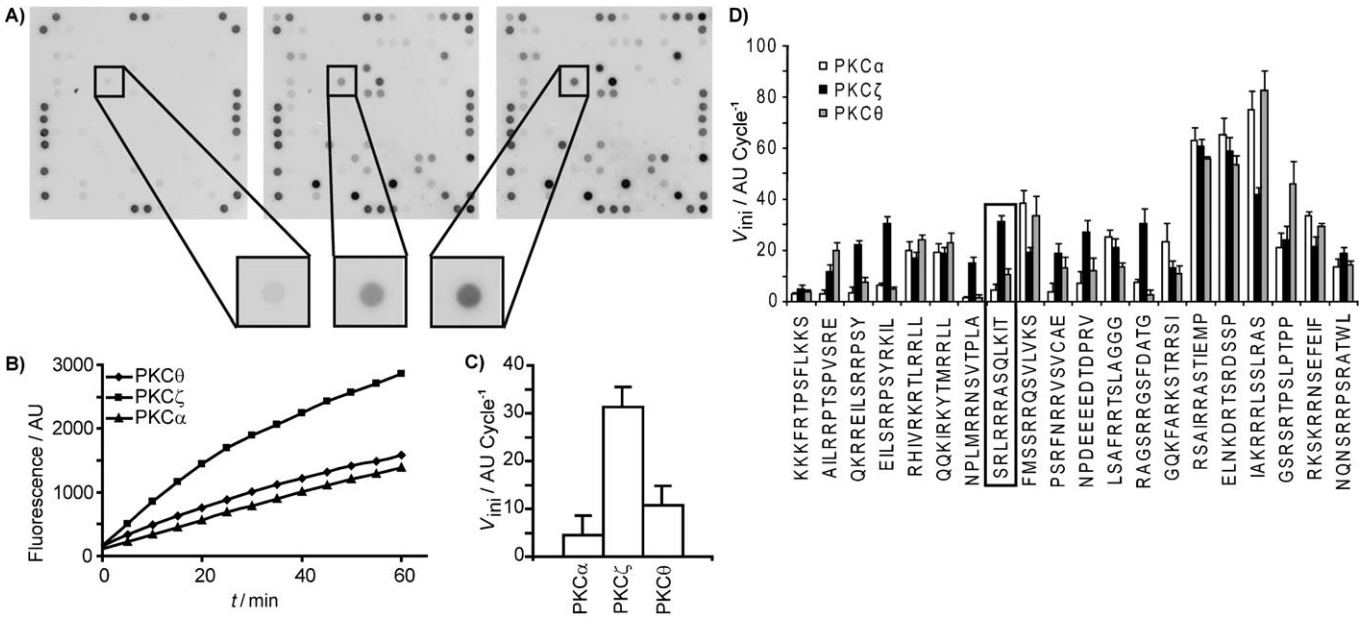

Figure 2. Selection of peptides with maximum PKC isozyme selectivity. A) Images of the microarray after 0, 30 and 60 min that show increasing fluorescence of substrate spots. B) Integrated fluorescence of the highlighted spot with sequence SRLRRRASQLKIT followed in time for the three isozymes used. C) Slopes of the curves for the highlighted spots showing clear differences in v_{ini} for this substrate. D) v_{ini} values for all phosphorylated substrates. Error bars indicate the standard error of the mean over three independent experiments, and the box marks the results for the spot highlighted in A).

Preparation of ATP-site inhibitor

For the ATP-binding site inhibitor part of the newly designed bisubstrate-based inhibitors, a functionalised bisindolyl maleimide was selected (**1**, Scheme 1). This compound bears a strong resemblance to a known kinase inhibitor that has a methyl group instead of the propargyl moiety and has already shown selectivity for PKCs compared to related kinases such as PKA and PKG.[24] These inhibitors are simplified mimics of the naturally occurring broad-spectrum kinase inhibitor staurosporine.[25] For subsequent attachment to peptides, the inhibitor was furnished with a propargyl group in such a way that the important basic trialkylamine moiety was maintained. Furthermore, it is known from crystal structure data of kinase–inhibi-

Table 1. Substrates phosphorylated by PKC on the microarray.

Sequence	Origin[a,b,c]	v_{ini} ratio α	ζ	θ	Sequence	Origin[a,b,c]	v_{ini} ratio α	ζ	θ
KKKFRTPSFLKKS	Beta-adducin 706–718 (P35612)[37]	1	2	1	NPDEEEEDTDPRV	cAMP-dependent protein kinase type II-α regulatory subunit 106–118 (P13861)	1	4	2
AILRRPTSPVSRE	32 kDa protein (E1A 13S protein) 212–224 (Q71BY8)	1	4	7	LSAFRRTSLAGGG	Myosin-binding protein cardiac type C 268–280 (Q14896)[41]	2	2	1
QKRREILSRRPSY	cAMP response element-binding protein 122–134 (P16220)[23]	1	7	2	RSGSRRGSFDATG	Desmoplakin 4635–4647 (P15924)	3	11	1
EILSRRPSYRKIL	cAMP response element-binding protein 126–138 (P16220)[23]	1	6	1	GQKFARKSTRRSI	Pleckstrin 106–118 (P08567)[42]	2	1	1
RHIVRKRTLRRLL	Epidermal growth factor receptor 671–683 (P00533)[38]	1	1	1	RSAIRRASTIEMP	Cardiac phospholamban 9–21 (P26678)	1	1	1
QQKIRKYTMRRLL	Receptor tyrosine-protein kinase erbB-2 precursor 679–691 (P04626)	1	1	1	ELNKDRTSRDSSP	Retinoblastoma-like protein 2 955–967 (Q08999)	1	1	1
NPLMRRNSVTPLA	6-phosphofructo-2-kinase/fructose-2,6-bisphosphatase 454–466 (Q16875)[39]	1	11	1	IAKRRRLSSLRAS	40S ribosomal protein S6 228–240 (P62753)	2	1	2
SRLRRRASQLKIT	GABA receptor subunit β-2 precursor 427–439 (P47870)[40]	1	7	2	GSRSRTPSLPTPP	Microtubule-associated protein tau 523–535 (P10636)[43]	1	1	2
FMSSRRQSVLVKS	Glutamate receptor ionotrope kainite 2 precursor 708–720 (Q13002)	2	1	2	RKSKRRNSEFEIF	Tryptophan 5-hydroxylase 1 51–63 (P17752)	2	1	1
SRFNRRVSVCAET	cAMP-dependent protein kinase type II-α regulatory subunit 91–103 (P13861)	1	5	3	NQNSRRPSRATWL	Vitronectin precursor 390–402 (P04004)	1	1	1

[a] References are to papers already describing the protein as a PKC substrate. [b] Ranges refer to the location of the peptide in the original protein. [c] In round brackets, protein references are to the Uni*P*rot KnowledgeBase.[44]

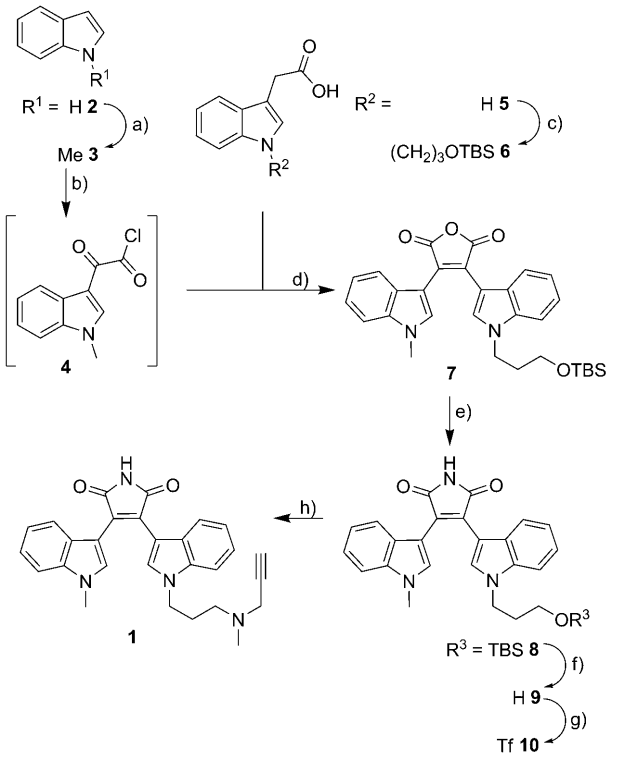

Scheme 1. Synthesis of the ATP site inhibitor **1**. a) MeI, NaH, THF, 0 °C, 100%; b) oxalyl chloride, CH_2Cl_2, 0 °C; c) $Br(CH_2)_3OTBS$, NaH, DMF, 89%; d) Et_3N, CH_2Cl_2, 20%; e) HMDS, MeOH, DMF, 91%; f) HCl, EtOH; g) Tf_2O, py, CH_2Cl_2, 0 °C; h) *N*-methyl-*N*-propargylamine **11**, CH_2Cl_2, 72% (over 3 steps).

tor complexes that the aromatic part of such inhibitors protrudes deeply into the ATP-binding pocket whereas the "tail", where the acetylene moiety is located, points towards the peptide-binding groove; this offers a convenient attachment point for the peptide part of a possible bisubstrate-based inhibitor.[16]

The synthesis (Scheme 1) was partly based on literature procedures.[24] First, indole **2** was alkylated with iodomethane in quantitative yield. Then, a maleimide precursor was introduced by Friedel–Crafts acylation of **3** with oxalyl chloride. The resulting acid chloride **4** was directly treated with indolyl acetic acid **6**, which was obtained by alkylation of acid **5**. Anhydride **7** was obtained in 20% yield. Subsequently, the maleimide was formed by reaction of **7** with hexamethyldisilazane (HMDS) in 91% yield. The *t*-butyldimethylsilyl (TBS) group of **8** was removed with acid, after which the free hydroxyl moiety of **9** was converted into triflate **10**, followed by substitution with commercially available *N*-methyl-*N*-propargylamine **11** to yield the desired inhibitor **1** in 72% yield.

Preparation of pseudosubstrates and bisubstrate-based inhibitors

The selected peptide EILSRRPSYRKIL was transformed into pseudosubstrates **12** and **13** (Scheme 2) by replacing the serine residue at the phosphorylation site with an alanine moiety and by introduction of a residue furnished with an azide moiety close to the phosphorylation site as an attach-

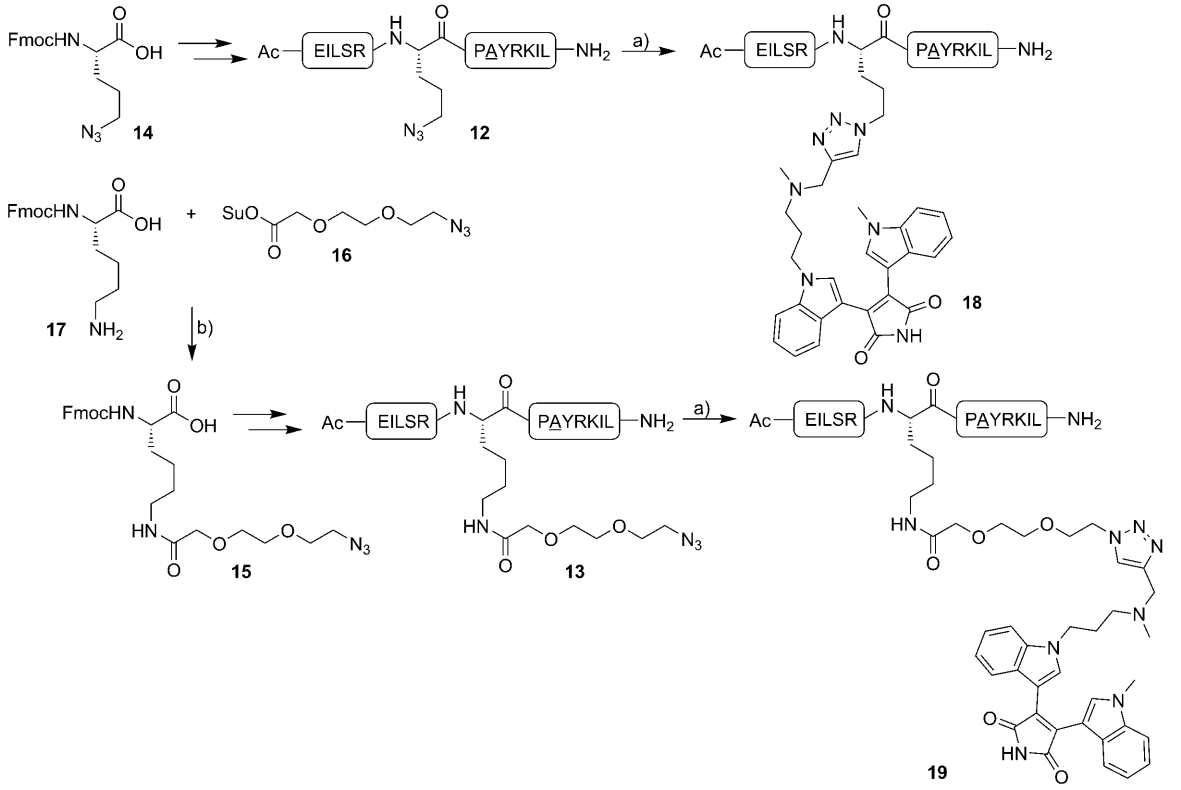

Scheme 2. Synthesis of bisubstrate inhibitors **18** and **19**. The alanine amino acid that replaces the phosphorylation site serine residue is underlined. a) ATP-binding-site inhibitor **1**, $CuSO_4$, sodium ascorbate, microwave, 80 °C. b) iPr_2EtN, THF, 84%.

ment point for ATP-binding site inhibitors. The peptide contains two serine residues, but only one of them is in a typical PKC substrate motif, and unsurprisingly, this particular residue is known to be phosphorylated by PKC isozymes.[23] This residue was therefore selected for replacement. Because the other serine residue probably cannot be phosphorylated by PKC it was left intact to mimic the original substrate as closely as possible. Peptide **12** comprised a δ-azido-ornithine building block **14**.[26] Ornithine was chosen to most closely resemble the length of the side-chain in the original substrate, which had an arginine at this position. The attachment point was selected on the basis of modelling experiments by using crystal structure data,[16a,27] which demonstrated that the side-chain at this position is directed towards the ATP-binding site and that the distance between the two binding sites at this location can be easily bridged. From the modelling experiments it was clear that the peptide groove extends in both directions from the ATP-binding site and therefore attachment of the ATP-binding site inhibitor in the middle of the peptide near the phosphorylation site should lead to maximum interaction in the resulting bisubstrate-based inhibitors. However, the convenient synthetic approach described here allows many different attachment configurations to be evaluated in the future. In addition, peptide **13** was prepared. It comprises a lysine functionalised with an ε-azido-oligoethyleneglycol spacer **15**, which was prepared by coupling of succinimidyl ester **16** to Fmoc-Lys-OH **17**. The peptides were prepared by using standard Fmoc/*t*Bu solid-phase chemistry on a Rink amide resin[28] to obtain C-terminal amides, and were obtained in good yields after purification.

Then, ATP-binding site inhibitor **1** was linked to peptides **12** and **13** by using a "click"-reaction mediated by $CuSO_4$ and sodium ascorbate (Scheme 2).[12] The microwave-assisted coupling was carried out at 80 °C for 20 min.[29] The resulting bisubstrates **18** and **19** were obtained in good yields (over 80%) after RP-HPLC purification. Analytical HPLC traces and MALDI-MS spectra for all peptides and bisubstrates are included in the Supporting Information.

Activity analysis of bisubstrate-based inhibitors

The inhibition activity and selectivity of the bisubstrate-based inhibitors was investigated by employing a similar microarray setup used for the original selection of substrates. A 96-well format was used, and in that way four inhibitors could be tested at various concentrations (10 nM up to 10 μM) in triplicate against an isozyme with positive controls (no inhibitor present) and negative controls (no ATP present) on one PamChip 96-array plate (layout given in the Supporting Information). A high ATP concentration (100 μM) was used in these experiments to give a strong fluorescent read-out. For these experiments, a new array was used that only contained a number of substrates that are efficiently phosphorylated by the PKC isozymes used.

For the inhibition experiments, substrates were monitored that showed good phosphorylation by the three isozymes in combination with one antiphosphoserine/antiphosphothreonine antibody: CREB1 (cAMP response element binding protein 126–138, EILSRRPSYRKIL), KPCB (PKC splice isoform β-II 19–31, RFARKGSLRQKNV), MARCS (myrostoylated alanine-rich C-kinase substrate 152–164, KKKKKRFSKKSF) and NCF1 (neutrophil cytosol factor 1 296–308, RGAPPRRSSIRNA).

In Figure 3, typical inhibition curves obtained by using this method are shown (full data are available as Supporting Information). By using the 96-array setup described above, a complete picture of the affinity and selectivity of all inhibitors could be obtained in one experiment. The results of the inhibition experiments are summarised in Table 2.

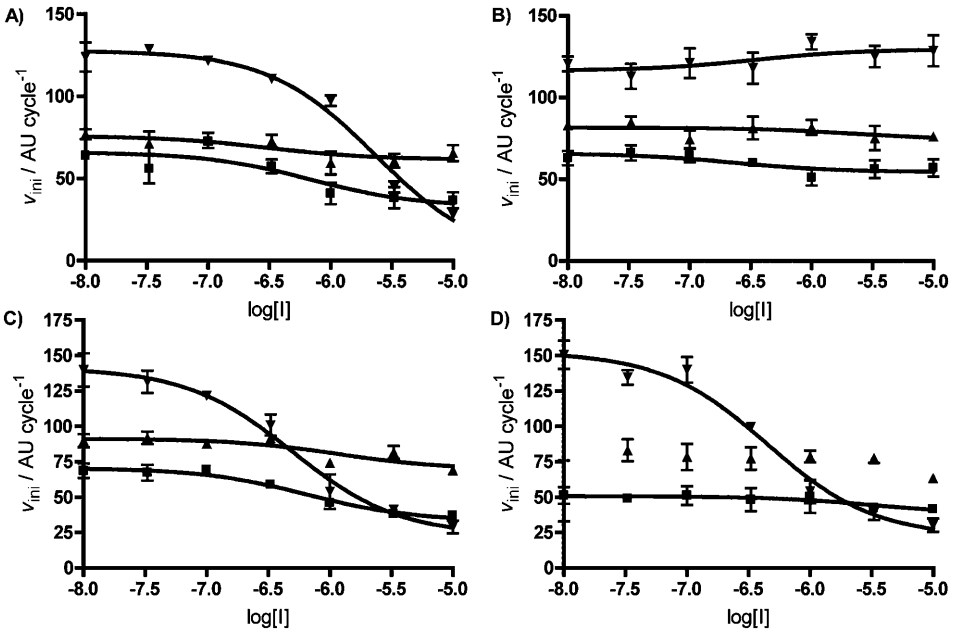

Figure 3. Representitive sample curves obtained in the inhibitor evaluation experiments. A) Staurosporine mimic **1**, B) Pseudosubstrate **12**, C) Bisubstrate-based inhibitor **18**, D) Bisubstrate-based inhibitor **19**. ■: PKCα, ▼: PKCθ, ▲: PKCζ.

From the data summarised in Table 2, it can be concluded that staurosporine mimic **1** (Figure 3A) causes decent inhibition (IC_{50} 2–4 μM) of PKCα and PKCθ, but no inhibition of PKCζ; this pattern is comparable to that of natural PKC inhibitor staurosporine. It should be noted that the IC_{50} values obtained with substrate NCF1 were higher, and in these cases poorly fitted curves were obtained, and consequently the

Table 2. Inhibition data bisubstrate inhibitors

		IC_{50} [μM][a] Inhibitor			
Enzyme	Substrate[b]	**1**	**12**	**18**	**19**
PKCα	CREB1	1.8±0.6	–	1.0±0.2	–
	KPCB	2.9±0.9	–	1.0±0.2	–
	MARCS	1.9±0.5	–	1.1±0.2	–
	NCF1	6.5±2.6	–	2.4±0.6	–
PKCζ	CREB1	–	–	–	–
	KPCB	–	–	–	–
	MARCS	–	–	–	–
	NCF1	–	–	–	–
PKCθ	CREB1	2.9±0.3	–	0.7±0.1	0.5±0.1
	KPCB	2.3±0.3	–	0.6±0.1	0.43±0.03
	MARCS	2.9±0.4	–	0.9±0.1	0.8±0.1
	NCF1	4.0±0.9	–	0.6±0.2	0.5±0.1

[a] If no value is given, no inhibition could observed below 10 μM. [b] CREB1 (cAMP response element binding protein 126–138, EILSRRPSYRKIL), KPCB (PKC splice isoform β-II 19–31, RFARKGSLRQKNV), MARCS (myristoylated alanine-rich C-kinase substrate 152–164, KKKKKRFSKKSF) and NCF1 (neutrophil cytosol factor 1 296–308, RGAPPRRSSIRNA).

errors are high. Therefore, for comparison only the data for substrates CREB1, KPCB and MARCS for which reliable inhibition curves could be obtained were used for further comparisons.

Clearly, pseudosubstrate **12** is not capable of inhibition at the concentrations tested (Figure 3B). On the other hand, the bisubstrate-based inhibitors were capable of inhibition (Figure 3C and D). The bisubstrate-based inhibitor without a spacer (**18**) shows similar inhibition of PKCα compared to ATP-binding site inhibitor **1** (IC_{50} 1.0–1.1 μM and 1.8–2.9 μM respectively). Its inhibition of PKCθ-mediated phosphorylation is significantly better (IC_{50}: 0.6–0.9 μM and 2.3–4.0 μM for **1**), and generally a fourfold reduction in the IC_{50} could be observed, and this afforded a high-nanomolar inhibitor. However, because the ATP concentration was high (100 μM) in these experiments, the IC_{50} values obtained will be significantly higher than the inhibition constants (K_i). Assuming our inhibitors are competitive (vide infra), the Cheng–Prusoff equation[30], $K_i = IC_{50}/(1+[S]/K_m)$, may be used to calculate a K_i from the IC_{50} value when the K_M for the original substrate, that is, ATP, is known. We determined the K_M of ATP for the PKCθ isozyme by using the peptide microarrays and varying the ATP concentrations in the absence of any inhibitor; this resulted in a K_M of 5 μM (data in Supporting Information). By taking this into account, a K_i of bisubstrate-based inhibitors **18** and **19** can be calculated as 20–40 nM versus 85–140 nM for ATP-site inhibitor **1**. The K_M obtained from these data is tenfold lower than a previously reported value from a different homogeneous assay (49 μM).[31] Using this higher value in the Cheng–Prusoff equation yields a K_i of 200–300 nM and 140–260 nM for inhibitors **18** and **19**, respectively.

Interestingly, bisubstrate-based inhibitor **19** did not significantly inhibit PKCα in contrast to bisubstrate-based inhibitor **18**; this demonstrates the importance of correct spacer length. Similar inhibition by **19** of PKCθ (IC_{50}: 0.4–0.8 μM) was observed as for bisubstrate-based inhibitor **18**. Clearly, bisubstrate-based inhibitor **19** has excellent isozyme selectivity for PKCθ amongst the three isoforms evaluated here. Selective inhibitors for PKCθ such as bisubstrate-based inhibitor **18** are particularly interesting because this kinase has been proposed as a drug target in human T cell leukaemias.[10] In the future, the approach described here can be extended to include all PKC isozymes, however because the current selectivity element was identified for a subset of three isozymes, it is likely that a different peptide part needs to be selected for selectivity amongst all PKC isozymes.

As a measure of assay quality in high-throughput screening, the Z′-factor has been introduced, which is reflective of both dynamic range and data variation.[32] This was above 0.5 (typically 0.6–0.8) for the various combinations of kinase and substrate employed here, except for the combination of PKCα and KPCB ($Z' = 0.4$). According to the criteria laid down in the original paper on the Z′-factor, this indicates that the microarray assay described here is well suited for high-throughput evaluation. A complete overview of the relevant Z′-factors is incorporated in the Supporting Information. An independent confirmation of the inhibition results was obtained by using the FRET-based solution-phase Z′-Lyte assay of Invitrogen. In Figure 4A the inhibition curves for bisubstrate-based inhibitor **19** with PKCα, -ζ and -θ are shown again by using an ATP concentration of 100 μM; this clearly demonstrates a similar selectivity profile as in the microarray experiments. It should be noted that in the FRET assay an IC_{50} of 60 nM was observed for inhibitor **19** with PKCθ. The IC_{50} values obtained in this way are approximately tenfold lower than the those obtained in the microarray assay. This might be due to the effect of immobilization of a substrate on enzyme kinetics in the microarray assay. Furthermore, a different peptide was used in the Z′-Lyte assay and from the microarray data shown it is clear that there might be a slight substrate dependence of inhibition with these bisubstrate-based inhibitors. However, this lower IC_{50} seems to indicate that the inhibitors described here are even more potent, and have a low-nanomolar K_i.

To determine the mechanism of inhibition of the bisubstrate-based inhibitors described here, experiments were carried out in which the phosphorylation kinetics were monitored as a function of inhibitor concentration for varying concentrations of either peptidic substrate or ATP. In fact, the dependence on peptidic substrate concentration could be conveniently evaluated from the dataset used to determine the IC_{50} values because each peptide on the microarray employed was spotted at different concentrations. This further demonstrates the power of microarrays to quickly obtain comprehensive information on kinase inhibitors. Thus, by plotting the reciprocal initial velocity as a function of the concentration of inhibitor **19** for different spot concentrations, a Dixon plot[33] could be constructed that showed a characteristic pattern for a peptide competitive inhibitor, that is, an intersection in the top-left quadrant (Figure 4B), with a K_i of 1.1 μM. A similar experiment was carried out at varying ATP concentrations (see the Supporting Information); this again afforded a Dixon plot characteristic of an ATP competitive inhibitor (Figure 4C and D), with a K_i of 80 nM.

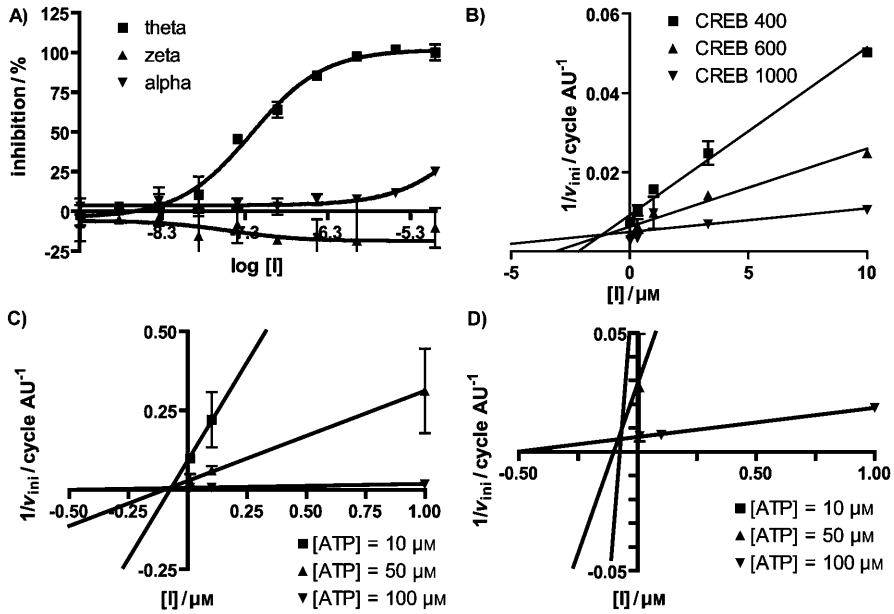

Figure 4. Solution-phase assay results and kinetic investigations. A) Inhibition curves obtained by using Invitrogen's Z′-Lyte assay for inhibitor **19**. B) Dixon plot obtained for inhibitor **19** and PKCθ in combination with different spot concentrations of the CREB1 peptide. C) Dixon plot obtained for inhibitor **19** and PKCθ with different ATP concentrations. D) Enlargement of the ATP Dixon plot showing the position of the intersection.

The increase in affinity for bisubstrate-based inhibitors **18** and **19** is modest compared to some of the earlier bisubstrate-based inhibitors.[6] However, the inhibitors described here have not yet been optimised with respect to, for instance, spacer length, and from the significant differences in IC_{50} values for these two inhibitors it is clear that spacer length is important. The convenient synthetic and analytical set-up described here will allow one to evaluate many compounds with variable spacer lengths. In addition, in these inhibitors an arginine residue, which is positively charged at physiological pH, was replaced by a building block that can no longer be protonated. This obviously might have impacted the binding affinity of the peptide part for PKC's binding groove, in particular because the arginine residue that was replaced is part of the PKC consensus sequence. Currently, work is being carried out on the introduction of arginine derivatives that have a handle amenable to click chemistry.

It should be noted that the selectivity towards isozyme PKCθ was not the same as the selectivity profile observed during the first selection, because the peptide used was selectively recognised by PKCζ. This might be due to differences in binding mode caused by attachment of the ATP-binding site inhibitor. In the bisubstrate-based inhibitors described here, a positively charged arginine residue was replaced by neutral building blocks. As stated before, the purpose of the initial screening was to find sequences displaying maximum differences in affinity, which therefore maximally exploit the minute differences in the kinases' peptide-binding grooves. A combinatorial approach employing these sequences might allow rapid preparation and evaluation of different combinations to obtain the desired selectivity.

To further determine the selectivity of bisubstrate-based inhibitor **19**, it was also tested for its ability to inhibit PKA, which is a kinase highly homologous to the PKC family. The peptide microarrays were again used to study inhibition of PKA by using similar conditions to those used in the PKC inhibition assay, with inhibitor concentrations of 0.33–10 μM (data shown in Supporting Information). No significant inhibition could be observed at these concentrations; this indicates further that bisubstrate inhibitor **19** has excellent selectivity.

All these results together demonstrate the power of the methodology presented here, because the developed bisubstrate-based inhibitors can give significant increases in both affinity and selectivity, even in challenging scenarios such as selectivity towards highly homologous isozymes. An exciting advantage of this strategy is the possibility to quickly screen in a comprehensive and statistically meaningful manner different combinations of components of potential inhibitors (i.e., pseudosubstrate part, ATP-binding site inhibitor moiety and spacer) against the enzymes of interest thereby providing a versatile, fragment-based approach. In addition, this methodology might allow the rapid discovery of lead bisubstrate-based inhibitors with good selectivity towards a kinase of interest.

Conclusions

A powerful methodology is described that allows the rapid development of bisubstrate-based kinase inhibitors with enhanced selectivity and affinity for a given set of substrates. The strategy employs dynamic peptide microarrays for finding substrate peptides with large affinity differences for the kinases of interest and for comprehensively evaluating bisubstrate-based inhibitors derived from those peptides. As a proof of principle, the experimental setup was employed to develop a bisubstrate inhibitor for PKCθ that showed good selectivity with respect to two highly homologous isozymes, PKCα and PKCζ. The resulting inhibitor showed both increased affinity and selectivity compared with its constituent parts. This strategy might allow the rapid discovery and optimization of selective bisubstrate kinase inhibitors.

Experimental Section

General: All reactions were carried out at ambient temperature unless stated otherwise. All reagents were used as supplied from

commercial sources unless stated otherwise. CH_2Cl_2, *N*-methylpyrrolidone (NMP) and iPr_2EtN were stored on molecular sieves (4 Å) prior to use. R_f values were determined by thin layer chromatography (TLC) on Merck precoated silicagel 60 F_{254} plates. Spots were visualised by UV-quenching, ninhydrin or Hanessian's stain (cerium molybdate). Column chromatography was carried out by using Silicycle UltraPure silica gel (40–63 μm). ^{1}H NMR spectra were recorded on a Varian G-300 (300 MHz) spectrometer and chemical shifts are given in ppm relative to tetramethylsilane (TMS, $\delta = 0.00$ ppm). ^{13}C NMR spectra were recorded by using the attached proton test (APT) sequence on a Varian G-300 (75.5 MHz) spectrometer and chemical shifts are given in ppm relative to TMS by using the residual proton signal in $CDCl_3$ ($\delta = 77.0$ ppm). Electrospray ionisation mass spectrometry was performed on a Shimadzu LCMS-QP8000 single-quadrupole bench-top mass spectrometer in positive-ionisation mode. MALDI-TOF mass spectrometry was performed on a Kratos CFR spectrometer. Preparative HPLC was carried out on a Gilson preparative HPLC system equipped with a reversed-phase C8 column (Alltech Altima XL C8, 100 Å, 10 μm, 250×22 mm) by using a linear gradient of 100% buffer A (0.1% TFA in H_2O/MeCN, 95:5; *v/v*) to 100% buffer B (0.1% TFA in H_2O/MeCN, 5:95; *v/v*) in 40 min at a flow rate of 11.5 mL min^{-1} Analytical HPLC was carried out on a Shimadzu HPLC workstation by using a reversed-phase C8 column (Altima XL C8, 90 Å, 5 μm, 250×4.6 mm, Alltech, Deerfield, IL, USA) by using a linear gradient of the same buffers as above in 20 min at a flow rate of 1.0 mL min^{-1} Microwave-assisted reactions were conducted in closed reaction vessels by using a Biotage (Uppsala, Sweden) Initiator microwave reactor equipped with a temperature and pressure sensor for monitoring reaction conditions.

1-Methyl-1*H*-indole 3:[35] Indole (**2**; 11.7 g, 100 mmol) was dissolved in freshly distilled THF and at 0 °C NaH (a 60% dispersion in mineral oil, 6.0 g, 150 mmol) was added. After 15 min MeI (18.8 g, 8.4 mL, 134 mmol) was added slowly, and the mixture was allowed to stir at RT for 60 min. The reaction was cooled to 0 °C, sat. aq NH_4Cl (400 mL) was added, and the mixture was extracted with Et_2O (3×100 mL). The combined organic layers were washed with 1 M $KHSO_4$ (3×150 mL), sat. aq $NaHCO_3$ (3×150 mL) and brine (150 mL). The organic phase was dried on $MgSO_4$, evaporated to dryness, and the crude product was purified by using column chromatography (EtOAc/hexanes, 1:4; *v/v*) yielding **3** (13 g, quant) as a clear, colourless liquid. $R_f = 0.68$ (EtOAc/hexanes, 1:2; *v/v*); ^{1}H NMR ($CDCl_3$, 300 MHz): $\delta = 7.62$ (dt, $^3J = 8.0$ Hz, 0.8 Hz, 1H), 7.31 (m, 1H), 7.21 (m, 1H), 7.10 (m, 1H), 7.01 (d, $^3J = 3.0$ Hz, 1H), 6.47 (dd, $^3J =$ 3.0, 0.8 Hz, 1H), 3.74 ppm (s, 3H); ^{13}C NMR ($CDCl_3$, 75.5 MHz): $\delta =$ 136.6 (*C*-Ar), 128.7 (*C*H-Ar), 128.4 (*C*-Ar), 121.4, 120.8, 119.2, 109.1, 100.8 (*C*H-Ar), 32.7 ppm (CH_3).

2-(1-(3-*tert*-Butyldimethylsilyloxypropyl)-1*H*-indol-3-yl) acetic acid 6: 2-(1*H*-Indol-3-yl) acetic acid (**5**; 3.5 g, 20 mmol) was dissolved in DMF (30 mL), cooled to 0 °C, and NaH (a 60% dispersion in mineral oil, 1.76 g, 44 mmol) was added. The mixture was stirred for 20 min, then 1-bromo-3-*tert*-butyldimethylsilylpropanol[34] (5.57 g, 22 mmol) was added slowly, and the mixture was stirred at RT for 3 h, then evaporated to dryness. Excess NaH was quenched by the addition of H_2O to the mixture. After addition of 1 M $KHSO_4$ (50 mL), the crude product was extracted with EtOAc (3×50 mL). The combined organic layers were dried on $MgSO_4$ and concentrated in vacuo. Purification by using column chromatography (CH_2Cl_2/HOAc, 99:1; *v/v*) yielded **6** (6.9 g, 89%) as an off-white oil. $R_f = 0.29$ (CH_2Cl_2/MeOH, 95:5; *v/v*); ^{1}H NMR ($CDCl_3$, 300 MHz): $\delta = 11.02$ (br s, 1H), 7.58 (d, $^3J = 7.7$ Hz, 1H), 7.30 (d, $^3J = 8.3$ Hz, 1H), 7.18 (m, 1H), 7.09 (m, 2H), 4.16 (t, $^3J = 6.7$ Hz, 2H), 3.75 (s, 2H), 3.52 (t, $^3J =$ 5.6 Hz, 2H), 1.94 (m, 2H), 0.92 (s, 9H), 0.04 ppm (s, 6H); ^{13}C NMR ($CDCl_3$, 75.5 MHz): $\delta = 178.4$ (COOH), 136.1, 127.6 (*C*-Ar), 127.1, 121.6, 119.1,118.9, 109.5 (*C*H-Ar), 105.9 (*C*-Ar), 59.4 (CH_2-O), 42.5 (CH_2N), 32.9 (CH_2-COOH), 31.0 (CH_2), 25.9 (Si-C(CH_3)$_3$), 18.2 (Si-*C*-(CH_3)$_3$), −5.5 ppm (Si-CH_3); elemental analysis calcd (%) for $C_{18}H_{27}NO_3Si$: C 64.83, H 8.16, N 4.20; found: C 64.69, H 8.10, N 4.25.

2-(1-(3-*tert*-Butyldimethylsilyloxypropyl)-1*H*-indol-3-yl)-3-(1-methyl-1*H*-indol-3-yl) maleic anhydride 7: A solution of 1-methyl-1*H*-indole (**3**; 1.31 g, 10 mmol) in CH_2Cl_2 (50 mL) was added dropwise to a solution of oxalyl chloride (3.8 mL, 5.1 g, 40 mmol) in CH_2Cl_2 (50 mL) at 0 °C, and after 30 min the reaction mixture was evaporated to dryness. The crude product was dissolved in dry CH_2Cl_2 (50 mL) and this solution was added dropwise to a solution of 2-(1-(3-*tert*-butyldimethylsilyloxypropyl)-1*H*-indol-3-yl)acetic acid **6** (3.5 g, 10 mmol) and Et_3N (3.03 g, 4.1 mL, 30 mmol) in CH_2Cl_2 (50 mL). The reaction mixture was stirred at RT for 3 h and then evaporated to dryness. The crude compound was dissolved in EtOAc (50 mL) and washed with 1 M $KHSO_4$ (3×25 mL), sat. aq $NaHCO_3$ (3×25 mL) and brine (25 mL). The organic layer was dried on $MgSO_4$, evaporated to dryness and purified by using column chromatography (EtOAc/hexanes, 1:4; *v/v*) yielding **7** (1.03 g, 20%) as a bright-red solid. $R_f = 0.55$ (EtOAc/hexanes, 1:2; *v/v*); ^{1}H NMR ($CDCl_3$, 300 MHz): $\delta = 7.77$ (s, 1H), 7.70 (s, 1H), 7.38 (d, $^3J = 8.2$ Hz, 1H), 7.31 (d, $^3J = 8.2$ Hz, 1H), 7.13 (m, 2H), 7.04 (d, $^3J = 8.0$ Hz, 1H), 6.81 (m, 2H), 6.74 (m, 1H), 4.28 (t, $^3J = 6.9$ Hz, 2H), 3.86 (s, 3H), 3.57 (t, $^3J = 5.6$ Hz, 2H), 1.99 (m, 2H), 0.92 (s, 9H), 0.05 ppm (s, 6H); ^{13}C NMR ($CDCl_3$, 75.5 MHz): $\delta = 166.9$, 166.7 (*C*=O), 136.9, 136.2 (*C*-Ar), 133.7, 132.9 (*C*H-Ar), 127.3, 125.9, 125.5 (*C*-Ar), 122.5, 122.3, 120.4, 109.9, 109.7 (*C*H-Ar), 105.1, 105.0 (*C*-Ar), 59.1 (CH_2O), 43.1 (CH_2), 33.3 (CH_3N), 32.6 (CH_2N), 25.8 (SiC(CH_3)$_3$), 18.1 (Si*C*(CH_3)$_3$), −5.5 ppm (Si-CH_3); elemental analysis calcd (%) for $C_{30}H_{34}N_2O_4Si$: C 70.01, H 6.66, N 5.44; found: C 70.20, H 6.71, N 5.29.

2-(1-(3-*tert*-Butyldimethylsilyloxypropyl)-1*H*-indol-3-yl)-3-(1-methyl-1*H*-indol-3-yl) maleimide 8: 2-(1-(3-*tert*-Butyldimethylsilyloxypropyl)-1*H*-indol-3-yl)-3-(1-methyl-1*H*-indol-3-yl) maleic anhydride (**7**; 1.0 g, 2 mmol) was dissolved in DMF (8 mL), a mixture of hexamethyldisilazane (4.2 mL, 20 mmol) and MeOH (0.4 mL, 10 mmol) was added, and the reaction was stirred at RT. After 24 h, H_2O (20 mL) was added, and the mixture was extracted with EtOAc (4×50 mL). The combined organic layers were dried on $MgSO_4$ and concentrated in vacuo. The crude product was purified by using column chromatography (EtOAc/hexanes, 1:4→1:2; *v/v*) yielding **8** (0.92 g, 91%) as a red solid. $R_f = 0.34$ (EtOAc/hexanes, 1:2; *v/v*); ^{1}H NMR ($CDCl_3$, 300 MHz): $\delta = 8.32$ (s, 1H), 7.68 (s, 1H), 7.59 (s, 1H), 7.29 (d, $^3J = 8.2$ Hz, 1H), 7.19 (d, $^3J = 8.2$ Hz, 1H), 7.03 (m, 3H), 6.71 (m, 3H), 4.19 (t, $^3J = 6.8$ Hz, 2H), 3.73 (s, 3H), 3.51 (t, $^3J = 5.5$ Hz, 2H), 1.92 (m, 2H), 0.89 (s, 9H), 0.01 ppm (s, 6H); ^{13}C NMR ($CDCl_3$, 75.5 MHz): $\delta = 172.7$, 172.5 (*C*=O), 136.7, 136.1 (*C*-Ar), 132.7, 131.8 (*C*H-Ar), 127.5, 127.4, 126.2, 125.9 (*C*-Ar), 122.1, 122.0, 199.9, 119.8, 109.6, 109.2 (*C*H-Ar), 105.8, 105.5 (*C*-Ar), 59.2 (CH_2O), 42.9 (CH_2), 33.1 (CH_3N), 32.8 (CH_2N), 25.8 (SiC(CH_3)$_3$), 11.5 (Si*C*(CH_3)$_3$), −5.5 ppm (SiCH_3); elemental anaylsis calcd (%) for $C_{30}H_{35}N_3O_3Si$: C 70.14, H 6.87, N 8.18; found: C 70.34, H 6.85, N 8.10.

2-(1-(3-Hydroxypropyl)-1*H*-indol-3-yl)-3-(1-methyl-1*H*-indol-3-yl) maleimide 9: 2-(1-(3-*tert*-Butyldimethylsilyloxypropyl)-1*H*-indol-3-yl)-3-(1-methyl-1*H*-indol-3-yl) maleimide (**8**; 382 mg, 0.75 mmol) was dissolved in 1% HCl in EtOH (20 mL) and stirred at ambient temperature for 1 h. The crude product was evaporated to dryness and purified over a silica column (EtOAc/hexanes, 1:1; *v/v*) yielding **9** (quant) as red crystals. $R_f = 0.25$ (EtOAc/hexanes, 2:1; *v/v*); ^{1}H NMR ($CDCl_3$, 300 MHz): $\delta = 10.92$ (s, 1H), 7.86 (s, 1H), 7.71 (s, 1H), 7.46 (d, $^3J = 8.2$ Hz, 1H), 7.42 (d, $^3J = 8.2$ Hz, 1H), 7.03 (t, $^3J =$

7.4 Hz, 2H), 6.90 (d, ^3J=8.0 Hz, 1H), 6.64 (m, 3H), 4.62 (t, ^3J=4.9 Hz, 1H), 4.27 (t, ^3J=6.7 Hz, 2H), 3.86 (s, 3H), 3.36 (m, 2H), 1.85 ppm (m, 2H); ^{13}C NMR ($CDCl_3$, 75.5 MHz): δ=172.9 (*C*=O), 136.5, 135.7 (*C*-Ar), 133.1, 131.9 (*C*H-Ar), 127.5, 126.7, 126.1, 125.5 (*C*-Ar), 121.6, 121.1, 119.4, 110.1 (*C*H-Ar), 104.9, 104.6 (*C*-Ar), 57.5 (CH_2OH), 42.7 (CH_2), 32.9 (CH_3N), 32.8 ppm (CH_2N); elemental analysis calcd (%) for $C_{24}H_{21}N_3O_3$: C 72.16, H 5.30; N 10.52; found: C 72.01, H 5.19, N 10.39.

2-(1-(3-(*N*-Methyl-*N*-propargylamino)propyl)-1*H*-indol-3-yl)-3-(1-methyl-1*H*-indol-3-yl) maleimide 1: 2-(1-(3-Hydroxypropyl)-1*H*-indol-3-yl)-3-(1-methyl-1*H*-indol-3-yl) maleimide (**9**; 50 mg, 0.125 mmol) and pyridine (10 mg, 10 μL, 0.125 mmol) were suspended in CH_2Cl_2 (2 mL) and cooled to 0 °C. Triflic anhydride (35 mg, 20 μL, 0.125 mmol) was added dropwise, and the reaction mixture was stirred at 0 °C for 45 min. *N*-Methyl-*N*-propargylamine (**11**; 17 mg, 21 μL, 0.25 mmol) was added, and the solution was stirred at RT for 3 h. The reaction mixture was evaporated to dryness, and the crude product was dissolved in EtOAc (5 mL) and washed with $KHSO_4$ (1 M, 3×10 mL), sat. aq $NaHCO_3$ (3×10 mL) and brine (10 mL). The organic layer was dried on $MgSO_4$ and concentrated in vacuo. The crude product was purified by using column chromatography (CH_2Cl_2/MeOH, 98:2; *v/v*) yielding **1** (35 mg, 72%) as a red solid. R_f=0.31 (CH_2Cl_2/MeOH, 95:5; *v/v*); ^{1}H NMR ($CDCl_3$, 300 MHz): δ=7.72 (s, 1H), 7.64 (s, 1H), 7.60 (s, 1H), 7.33 (d, ^3J=8.2 Hz, 1H), 7.27 (d, ^3J=7.2 Hz, 1H), 7.06 (m, 3H), 6.74 (m, 3H), 4.21 (t, ^3J=6.6 Hz, 2H), 3.84 (s, 3H), 3.31 (d, ^3J=2.5 Hz, 2H), 2.36 (t, ^3J=6.6 Hz, 2H), 2.21 (s, 3H), 2.20 (t, ^3J=2.2 Hz, 1H), 1.94 ppm (m 2H); ^{13}C NMR ($CDCl_3$, 75.5 MHz): δ=172.3, 172.1 (*C*=O), 136.8, 136.1 (*C*-Ar), 132.8, 131.9 (*C*H-Ar), 127.7, 127.5, 126.5, 126.0 (*C*-Ar), 122.2, 120.0, 109.6, 109.3 (*C*H-Ar), 105.8, 105.6 (*C*-Ar), 78.3 (*C*≡CH), 73.3 (C≡*C*H), 51.8 (CH_2N), 45.6 (CH_2N), 44.0 (CH_2N), 33.3 (CH_3N), 29.7 (CH_3N), 27.5 ppm (CH_2); elemental analysis calcd (%) for $C_{28}H_{26}N_4O_2$: C 74.65, H 5.82, N 12.44; found: C 74.52, H 5.90, N 12.57.

General procedure peptide synthesis: The peptide was prepared on Tentagel S RAM resin on a 0.25 mmol scale by using Fmoc/*t*Bu solid-phase chemistry. Agitation was achieved by bubbling with N_2. *Fmoc-deprotection*: The resin was treated with 20% piperidine in DMF (5.0 mL, 3×8 min), followed by washing with DMF (5.0 mL, 3×2 min) and CH_2Cl_2 (5.0 mL, 3×2 min). A positive Kaiser-test[36] indicated successful deprotection. *Coupling*: The resin was treated with a solution of Fmoc-Xxx-OH (1.0 mmol), *O*-benzotriazole-*N*,*N*,*N*′,*N*′-tetramethyluroniumhexafluorophosphate (HBTU; 1.0 mmol), 1-hydroxybenzotriazol (HOBt; 1.0 mmol) and *i*Pr_2EtN (2.0 mmol) in DMF (5.0 mL) for 30 min. The resin was washed with DMF (5.0 mL, 3×2 min) and CH_2Cl_2 (5.0 mL, 3×2 min). A negative Kaiser-test indicated successful coupling. *Capping*: The resin was treated with a solution of Ac_2O (0.5 M), *i*Pr_2EtN (0.125 M) and HOBt·H_2O (0.015 M) in DMF (5.0 mL, 2×10 min). The resin was washed with DMF (5.0 mL, 3×2 min) and CH_2Cl_2 (5.0 mL, 3×2 min). A negative Kaiser-test indicated successful capping. *Cleavage and deprotection*: The resin was stirred with a mixture of trifluoroacetic acid (TFA; 9.5 mL), triisopropylsilane (TIS; 0.25 mL) and H_2O (0.25 mL) for 4 h at RT, after which it was removed by filtration and rinsed with TFA (3.0 mL). The crude peptide was precipitated from the combined filtrate by dropwise addition to a cold (−20 °C) mixture of methyl *t*-butyl ether and hexanes (40 mL, 1:1, *v/v*). After centrifugation (3000 rpm, 5 min) and decantation, the pellet was washed with Et_2O (3×40 mL). The resulting crude peptide was dissolved in H_2O and lyophilised.

Pseudosubstrate 12: The peptide was synthesised according to the General Procedure. After preparative HPLC and lyophilization, peptide **12** (130 mg, 31%) was obtained as a white powder. MALDITOF-MS: *m/z*: calcd for $C_{74}H_{127}N_{24}O_{18}$: 1640.0; found: 1640.2 $[M+H]^+$.

Pseudosubstrate 13: The peptide was synthesised according to General Procedure. After preparative HPLC and lyophilisation, peptide **13** (80 mg, 18%) was obtained as a white powder. MALDI-TOF-MS: *m/z*: calcd for $C_{102}H_{153}N_{28}O_{20}$: 1799.1; found: 1800.0 $[M+H]^+$.

Bisubstrate based inhibitor 18: Peptide **12** (3.0 mg, 1.8 μmol), $CuSO_4$·5H_2O (0.5 mg, 1.8 μmol), staurosporine mimic **1** (0.8 mg, 1.8 μmol) and sodium ascorbate (0.4 mg, 1.8 μmol) were dissolved in 1:1 (*v/v*) *t*-BuOH/H_2O (1.0 mL). The resulting reaction mixture was heated under microwave irradiation to 80 °C for 20 min. After lyophilization, the peptide was purified by preparative HPLC. Lyophilization of pure fractions afforded **18** (3.2 mg, 84%) as a white powder. MALDITOF-MS: *m/z*: calcd for $C_{81}H_{140}N_{25}O_{21}$: 2090.2; found: 2091.0 $[M+H]^+$.

Bisubstrate based inhibitor 19: Peptide **13** (2.0 mg, 1.1 μmol), $CuSO_4$·5H_2O (0.3 mg, 1.1 μmol), staurosporine mimic **1** (0.5 mg, 1.1 μmol) and sodium ascorbate (0.2 mg, 1.1 μmol) were dissolved in 1:1 (*v/v*) *tert*-BuOH/H_2O (1.0 mL). The reaction mixture was heated under microwave irradiation to 80 °C for 20 min. After lyophilization, the peptide was purified by preparative HPLC. Lyophilization of pure fractions afforded **19** (2.1 mg, 84%) as a white powder. MALDITOF-MS: *m/z*: calcd for $C_{109}H_{166}N_{29}O_{23}$: 2249.3; found: 2249.3 $[M+H]^+$.

Substrate profiling: A solution (25 μL) was used that contained 0.125 mg mL^{-1} kinase (20 ng), 3-*sn*-phosphatidyl-L-serine (Fluka BioChemika, St. Louis, MO, USA), Abl reaction buffer (50 mM Tris/HCl pH 7.5, 10 mM $MgCl_2$, 1 mM EGTA, 2 mM DTT, 0.01% Brij35; New England Biolabs, Ipswich, MA, USA) and 0.1 mg mL^{-1} BSA solution (New England Biolabs). The primary antiphosphoserine/antiphosphothreonine antibodies #2351, #9611 and #9391 (Cell Signalling Technology, Danvers, MA, USA), secondary fluorescent antibodies goat-antirabbit IgG-FITC (4 μg mL^{-1}) and goat-antimouse IgG-FITC (4 μg mL^{-1}; Santa Cruz Biotechnology, Santa Cruz, CA, USA) were incubated with 100 μM ATP. Samples were placed on the PamChip 4 STK-array chip (Pamgene, 's-Hertogenbosch, The Netherlands) and during 60 min incubation at 30 °C, real time images were taken automatically every 2.5 min. All images were analysed by BioNavigator software (Pamgene) and fluorescent intensities were expressed in arbitrary units.

Inhibitor evaluation: One 96-well plate was used for each kinase. The inhibitor of interest was dissolved in DMSO after which serial dilutions were made in 20% aq DMSO at 10× the final concentrations. Then H_2O (6.25 μL), a 0.5 mg mL^{-1} solution of phosphatidylserine (Fluka BioChimika) in H_2O (10 μL), Abl buffer (New England Biolabs; 2.5 μL), a 0.1 mg mL^{-1} solution of BSA (New England Biolabs) in H_2O (0.25 μL), a solution of antiPKA antibody #2261 (Cell Signalling Technologies) in buffer (0.25 μL), a 4 μg mL^{-1} solution of FITC-labelled goat-antirabbit antibody (Santa Cruz Biotechnology) in buffer (0.25 μL), and kinase (20 ng; Invitrogen) in buffer (0.5 μL) were added to all 96 wells. The inhibitor solution or 20% aq DMSO for the positive controls (2.5 μL) were added as well as a 1 mM solution of ATP in H_2O, or H_2O for the negative controls (2.5 μL). All inhibitor concentrations were tested in triplicate for each isozyme. The resulting plate layout is shown in the Supporting Information. Samples were placed on the PamChip 96 STK-array plate (Pamgene) and during 60 min incubation at 30 °C, real-time images were taken automatically every 2.5 min. All images were analysed

by BioNavigator software (Pamgene) and fluorescent intensities were expressed in arbitrary units.

Acknowledgements

The Netherlands Proteomics Centre (NPC, The Netherlands) is acknowledged for funding. Dr. J. H. Ippel is acknowledged for assistance with modelling experiments.

Keywords: bisubstrate-based inhibitors · combinatorial chemistry · enzymes · peptide microarrays · protein kinase C

[1] a) P. Cohen, *Nat. Rev. Drug Discovery* **2002**, *1*, 309; b) M. A. Arslan, O. Kutuk, H. Basaga, *Curr. Cancer Drug Targets* **2006**, *6*, 623; c) C. Naula, M. Parsons, J. C. Mottram, *Biochim. Biophys. Acta Proteins Proteomics* **2005**, *1754*, 151.
[2] J. Becker, *Nat. Biotechnol.* **2004**, *22*, 15.
[3] M. W. Karaman, S. Herrgard, D. K. Treiber, P. Gallant, C. E. Atteridge, B. T. Campbell, K. W. Chan, P. Ciceri, M. I. Davis, P. T. Edeen, R. Faraoni, M. Floyd, J. P. Hunt, D. J. Lockhart, Z. V. Milanov, M. J. Morrison, G. Pallares, H. K. Patel, S. Pritchard, L. M. Wodicka, P. P. Zarrinkar, *Nat. Biotechnol.* **2008**, *26*, 127.
[4] a) M. A. Bogoyevitch, R. K. Barr, A. J. Ketterman, *Biochim. Biophys. Acta Proteins Proteomics* **2005**, *1754*, 79; b) M. G. Kazanietz, L. B. Areces, A. Bahador, H. Mischak, J. Goodnight, J. F. Mushinski, P. M. Blumberg, *Mol. Pharmacol.* **1993**, *44*, 298.
[5] a) A. D. Broom, *J. Med. Chem.* **1989**, *32*, 2; b) A. Radzicka, R. Wolfenden, *Methods Enzymol.* **1995**, *249*, 284; c) K. Parang, P. A. Cole, *Pharmacol. Ther.* **2002**, *93*, 145.
[6] a) A. Ricouart, J. C. Gesquiere, A. Tartar, C. Sergheraert, *J. Med. Chem.* **1991**, *34*, 73; b) H. Räägel, M. Lust, A. Uri, M. Pooga, *FEBS J.* **2008**, *275*, 3608; c) E. Enkvist, G. Raidaru, A. Vaasa, T. Pehk, D. Lavogina, A. Uri, *Bioorg. Med. Chem. Lett.* **2007**, *17*, 5336; d) M. Loog, A. Uri, G. Raidaru, J. Järv, P. Ek, *Bioorg. Med. Chem. Lett.* **1999**, *9*, 1447.
[7] A. C. Hines, P. A. Cole, *Bioorg. Med. Chem. Lett.* **2004**, *14*, 2951.
[8] a) K. Parang, J. H. Till, A. J. Ablooglu, R. A. Kohanski, S. R. Hubbard, P. A. Cole, *Nat. Struct. Biol.* **2001**, *8*, 37; b) A. C. Hines, K. Parang, R. H. Kohanski, S. R. Hubbard, P. A. Cole, *Bioorg. Chem.* **2005**, *33*, 285.
[9] S. C. Meyer, C. D. Shomin, T. Gaj, I. Ghosh, *J. Am. Chem. Soc.* **2007**, *129*, 13812.
[10] J. H. Lee, S. Kumar, D. S. Lawrence, *ChemBioChem* **2008**, *9*, 507.
[11] A. Kumar, Y. Wang, X. Lin, G. Sun, K. Parang, *ChemMedChem* **2007**, *2*, 1346.
[12] a) V. V. Rostovtsev, L. G. Green, V. V. Fokin, K. B. Sharpless, *Angew. Chem.* **2002**, *114*, 2708; *Angew. Chem. Int. Ed.* **2002**, *41*, 2596; b) C. W. Tornøe, C. Christensen, M. Meldal, *J. Org. Chem.* **2002**, *67*, 3057.
[13] a) R. van Beuningen, H. van Damme, P. Boender, N. Bastiaensen, A. Chan, T. Kievits, *Clin. Chem.* **2001**, *47*, 1931; b) S. Lemeer, C. Jopling, F. Naji, R. Ruijtenbeek, M. Slijper, A. J. R. Heck, J. den Hertog, *PloS One* **2007**, *2*, e581; c) S. Lemeer, R. Ruijtenbeek, M. W. H. Pinkse, C. Jopling, A. J. R. Heck, J. den Hertog, M. Slijper, *Mol. Cell. Proteomics* **2007**, *6*, 2088; d) R. Hilhorst, L. Houkes, A. van den Berg, R. Ruijtenbeek, *Anal. Biochem.* **2009**, *387*, 150.
[14] J. M. Lord, J. Pongracz, *J. Clin. Pathol.* **1995**, *48*, M57.
[15] A. Altman, M. Villalba, *Curr. Cancer Drug Targets* **2002**, *2*, 125.
[16] a) Z.-B. Xu, D. Chaudhary, S. Olland, S. Wolfrom, R. Czerwinski, K. Malakian, L. Lin, M. L. Stahl, D. Joseph-McCarthy, C. Benander, L. Fitz, R. Greco, W. S. Somers, L. Mosyak, *J. Biol. Chem.* **2004**, *279*, 50401; b) N. Grodsky, Y. Li, D. Bouzida, R. Love, J. Jensen, B. Nodes, J. Nonomiya, S. Grant, *Biochemistry* **2006**, *45*, 13970; c) A. Messerschmidt, S. Macieira, M. Velarde, M. Badeker, C. Benda, A. Jestel, H. Brandstetter, T. Neuefeind, M. Blaesse, *J. Mol. Biol.* **2005**, *352*, 918.
[17] L. A. Selbie, C. Schmitz-Peiffer, Y. Sheng, T. J. Biden, *J. Biol. Chem.* **1993**, *268*, 24296.
[18] K. M. Conricode, K. A. Brewer, J. H. Exton, *J. Biol. Chem.* **1992**, *267*, 7199.
[19] J. H. Myklebust, E. B. Smeland, D. Josefsen, M. Sioud, *Blood* **2000**, *95*, 510.
[20] T. C. Sacktor, P. Osten, H. Valsamis, X. L. Jiuang, M. U. Naik, E. Sublette, *Proc. Natl. Acad. Sci. USA* **1993**, *90*, 8342.
[21] P. Martin, A. Duran, S. Minguet, M.-L. Gaspar, M.-T. Diaz-meco, P. Rennert, M. Leitges, J. Moscat, *EMBO J.* **2002**, *21*, 4049.
[22] K. Nishikawa, A. Toker, F.-J. Johannes, S.-Y. Zhou, L. C. Cantley, *J. Biol. Chem.* **1997**, *272*, 952.
[23] E. E. Solomou, Y. T. Juang, G. C. Tsokos, *J. Immunol.* **2001**, *166*, 5665.
[24] a) D. Toullec, P. Pianetti, H. Coste, P. Bellevergue, T. Grand-Perret, M. Ajakane, V. Baudet, P. Boissin, E. Boursier, F. Loriolle, L. Duhamel, D. Charon, J. Kirilovsky, *J. Biol. Chem.* **1991**, *266*, 15771; b) J. Kleinschroth, J. Hartenstein, C. Rudolph, C. Schächtele, *Bioorg. Med. Chem. Lett.* **1995**, *5*, 55; c) P. D. Davis, L. H. Elliott, W. Harris, C. H. Hill, S. A. Hurst, E. Keech, M. K. H. Kumar, G. Lawton, J. S. Nixon, S. E. Wilkinson, *J. Med. Chem.* **1992**, *35*, 994.
[25] a) T. Tamaoki, H. Nakano, *Bio/Technology* **1990**, *8*, 732; b) S. Omura, Y. Iwai, A. Hirano, A. Nakagawa, J. Awaya, H. Tsuchiya, Y. Takahashi, R. Asuma, *J. Antibiot.* **1977**, *30*, 275.
[26] M. Roice, I. Johannsen, M. Meldal, *QSAR Comb. Sci.* **2004**, *23*, 662.
[27] D. R. Knighton, J. H. Zheng, L. F. ten Eyck, V. A. Ashford, N. H. Xuong, S. S. Tayler, J. M. Sowadski, *Science* **1991**, *253*, 407.
[28] H. Rink, *Tetrahedron Lett.* **1987**, *28*, 3787.
[29] a) D. T. S. Rijkers, G. W. van Esse, R. Merkx, A. J. Brouwer, H. J. F. Jacobs, R. J. Pieters, R. M. J. Liskamp, *Chem. Commun. (Cambridge)* **2005**, 4581; b) J. A. F. Joosten, N. T. H. Tholen, F. Ait El Maate, A. J. Brouwer, G. W. van Esse, D. T. S. Rijkers, R. M. J. Liskamp, R. J. Pieters, *Eur. J. Org. Chem.* **2005**, 3182.
[30] Y. Cheng, W. H. Prusoff, *Biochem. Pharmacol.* **1973**, *22*, 3099.
[31] R. Czerwinski, A. Aulabaugh, R. M. Greco, S. Olland, K. Malakian, S. Wolfrom, L. Lin, R. Kriz, M. Stahl, Y. Huang, L. Piu, D. Chaudhary, *Biochemistry* **2005**, *44*, 9563.
[32] J.-H. Zhang, T. D. Y. Chung, K. R. Oldenburg, *J. Biomol. Screening* **1999**, *4*, 67.
[33] M. Dixon, *Biochem. J.* **1953**, *55*, 170.
[34] S. R. Wilson, P. A. Zucker, *J. Org. Chem.* **1988**, *53*, 4682.
[35] A. D. Kong, X. L. Han, X. Y. Lu, *Org. Lett.* **2006**, *8*, 1339.
[36] E. Kaiser, R. L. Colescott, C. D. Bossinger, P. I. Cook, *Anal. Biochem.* **1970**, *34*, 595.
[37] Y. Matsuoka, C. A. Hughes, V. Bennet, *J. Biol. Chem.* **1996**, *271*, 25157.
[38] K. A. Lund, C. S. Lazar, W. S. Chen, B. J. Walsh, J. B. Welsh, J. J. Herbst, G. M. Walton, M. G. Rosenfeld, G. N. Gill, H. S. Wiley, *J. Biol. Chem.* **1990**, *265*, 20517.
[39] M. H. Rider, J. van Damme, D. Vertommen, A. Michel, J. Vandekerckhove, L. Hue, *FEBS Lett.* **1992**, *310*, 139.
[40] B. J. Krishek, X.-M. Xie, C. Blackstone, R. L. Huganir, S. J. Moss, T. G. Smart, *Neuron* **1994**, *12*, 1081.
[41] L. Xiao, Q. Zhao, Y. Du, C. Yuan, R. J. Solaro, P. M. Buttrick, *Biochemistry* **2007**, *46*, 7054.
[42] K. L. Craig, C. B. Harley, *Biochem. J.* **1996**, *314*, 937.
[43] I. Correas, J. Diaznido, J. Avila, *J. Biol. Chem.* **1992**, *267*, 15721.
[44] The UniProt Consortium, *Nucleic Acids Res.* **2008**, *36*, D190.

Received: April 1, 2009
Published online on July 17, 2009

